JOURNAL OF MATERIALS SCIENCE: MATERIALS IN MEDICINE 7 (1996) 629–636

Preparation and properties of binary oxide bioceramics

S. AGATHOPOULOS*, P. NIKOLOPOULOS*, A. SALOMONI‡, A. TUCCI‡, I. STAMENKOVIC‡
*Chemical Engineering Dept., University of Patras and Institute of Chemical Engineering and High Temperature Chemical Processes, GR-265 00, Patras, Greece
‡Italian Ceramic Centre, Via Martelli 26, I-40138 Bologna, Italy

Candidate inert bioceramics based on Al_2O_3 and ZrO_2 and on SiO_2–TiO_2 were prepared via slip casting and sol–gel/hot-pressing techniques, respectively. Their properties relevant to applicability in biomedicine – microstructure, microhardness and coefficient of thermal expansion – were determined. The affinity of the oxides with body-liquids was evaluated by wetting experiments at 37 °C. High-quality materials were achieved due to the advantages offered by the preparation techniques employed. The Al_2O_3 and ZrO_2 based ceramics have high hardness, a constant coefficient of thermal expansion within a wide temperature range and low adhesion with biological liquids. The SiO_2–TiO_2 samples, the crystallinity of which depends on the preparation conditions, have lower hardness and lower coefficient of thermal expansion, which in the case of crystalline samples considerably changes at low temperatures, and display good affinity with biological liquids, strongly affected by the presence of glassy phase in the oxide.

1. Introduction

Ceramic materials have progressively attracted interest in the field of biomedicine, especially in long-term hard tissue implantations such as total joint replacements and dental implants, partly replacing metals and polymers [1–3]. Inert bioceramics [1] overcome the deficiencies of metals (corrosion) and polymers (degradation), providing remarkable chemical stability, tolerance in the body environment [2], high corrosion resistance, wear resistance, and sufficient mechanical strength [4], without exhibiting cytotoxic effects [5].

Materials which are found to be biocompatible [6] may not meet other requirements. For example, inert bioceramics such as aluminum oxide and titanium oxide are accepted by bones both in the jaw and joints. In special bioglasses, silicon oxide provides suitable surface compositions that are able to immobilize biomolecules in sensitive biological tests [1]. Recently, zirconium oxide has been introduced in orthopaedy [7], mainly because of its good mechanical properties [8], although its radioactivity [9] and degradation in the body environment [10] are subjects of current investigations.

Nevertheless, monolithic ceramics are rigid and inclined to brittle fracture. Therefore, the development of composites able to overcome this deficiency by combining a biocompatible material with other materials arises as one of the attractive objectives in the technology of biomaterials [11]. Furthermore, a composite material possibly enables better simulation of the mechanical properties of natural hard tissues [3].

Such a composite could be realized either by use of similar materials (i.e. ceramic/ceramic) or dissimilar ones (i.e. ceramic/metal). In the first case, the transformation toughening of zirconia ceramics is rapidly advancing in both scientific and technological fields [12]. In the case of ceramic/metal composites, literature data [13–15] support the idea that additions of oxides such as TiO_2 to a matrix of known biocompatible oxides will improve the weak adherence [13, 16] between ceramics and pure metals, resulting in a strong ceramic/metal interface [11].

In conclusion, although oxides such as those mentioned above are already known by their use in several applications, thorough studies are indispensable whenever they are proposed for biomedical applications in order to fulfill the special requirements of biomaterials previously outlined, i.e. long-term biocompatibility and biofunctionality in the body. Therefore, in this work the preparation and characterization– microstructure, hardness, thermal expansion, interactions with body liquids – of binary oxide ceramics are presented and discussed with emphasis on their adaptability in biomedicine. Two main approaches were followed:

(1) The production of mixed alumina (A)–(TZP) zirconia (Z) ceramics using a colloidal shaping procedure (slip casting) and sintering. This approach was chosen with the objective of eliminating the deleterious effects of hard agglomerates, limited packing levels and inadequate interparticle contacts in the ceramic microstructure and characteristics. In

0957–4530

order to obtain a better understanding of the possible effects of the preparation procedure studied, samples of pure alumina and (TZP) zirconia were also prepared and analysed from the point of view of international standards.

(2) Application of the sol–gel procedure to the production of SiO_2–TiO_2 (ST) powders and their subsequent hot pressing. Up until now, the binary SiO_2–TiO_2 system has been studied mainly in regard to technological applications in the field of glass-making due to the very low thermal expansion of this composition over a wide temperature range. Because of the positive biocompatible characteristics of both silica and titania, these oxides can be considered as candidate biomaterials.

2. Materials and experimental procedure

2.1. Preparation of samples

2.1.1. Densification of alumina–zirconia ceramics by slip casting and sintering

High-tech powders with high chemical purity over 99.5 wt% were employed to assure that potential applications in the biomedical field would not be jeopardized. Physical characterization of the powders was done using X-ray diffraction (XRD) analysis (Philips, Model 1820/00, Holland) to determine the crystal structure, the BET method (Quantachrome, Model Monosorb, USA) for surface area determinations and scanning electron microscopy (SEM) (JEOL, Model T330, Japan). An image analyser was used to determine the dimensions of agglomerates, unit particles and grains. The results obtained are reported in Table I.

According to SEM observations, all powders were in the form of spherical agglomerates ranging from 10 to 100 μm. It should be noted that this technique does not provide information about the origin or strength of the agglomerates. The rounded unit particles of the powders with small mean diameters (maximum of 0.3 μm) demonstrate high sinterability and expected high levels of sintering shrinkage.

TABLE I Characteristics of alumina–zirconia starting powders

Powder	Composition	Mean crystallite size (zirconia) (nm)	Surface area (m^2/g)	Mean unit particle (μm)
Mixed A–Z oxides				
2Z8A[a]	Y_2O_3 stabil. ZrO_2 with 80wt% Al_2O_3	27.0	9.5	ZrO_2:0.1 Al_2O_3:0.4
4Z6A[a]	Y_2O_3 stabil. ZrO_2 with 60wt% Al_2O_3	24.0	11.5	ZrO_2:0.1 Al_2O_3:0.3
6Z4A[a]	Y_2O_3 stabil. ZrO_2 with 40wt% Al_2O_3	22.0	14	ZrO_2:0.1 Al_2O_3:0.3
8Z2A[a]	Y_2O_3 stabil. ZrO_2 with 20wt% Al_2O_3	25.9	16	ZrO_2:0.1 Al_2O_3:0.3
Single oxides				
A[b]	α-alumina		10	0.16
Z[a]	Y_2O_3 stabil. ZrO_2	35.9	6	0.3

[a] Powders produced by TOSOH (Japan), (Z: 3 mol % Y_2O_3 partial stabilized zirconia)

[b] Powders produced by Baikowski, (France)

The mixed powders were homogenous mixtures consisting of very fine zirconia particles less than 0.1 μm in diameter together with alumina particles 0.3 μm in diameter. The surface area of the 8Z2A powder was the highest of all the powders studied, due to the highest percentage of zirconia. The unit particle sizes of the pure alumina and zirconia powders studied here as reference materials were also submicronic with a narrow size distribution.

Preparation of the dense ceramics consisted of wet milling the starting powders to reduce to a minimum level, if not to eliminate, agglomerates and to disperse the powder particles down to colloidal level. The mixture of "as received" powders, deionized water and organic deflocculant without alcalies was homogenized in a centrifugal mill with a zirconia jar and balls and a milling time of over 30 min. The investigated slips containing 21–33 vol % of solids and 0.5–1.8 wt % of polycarboxilic acid as deflocculant were characterized by low viscosities reflecting the high dispersion levels of the solids. The slip was cast in gypsum moulds to produce discs 28 mm in diameter with thickness up to 8 mm. The densities of the discs produced (see Section 2.2) are given in Table II. SEM examination of the cast green discs showed high homogeneity and limited presence of agglomerate fragments less than 5 μm in size.

The green samples were sintered in air with the following thermal cycle: heating to 800 °C at 1 °C/min and soaking at 800 °C for 1 h, heating to 1500 °C at 3 °C/min (1550 °C for 2Z8 A) and soaking at the maximum temperature for 2 h and finally cooling to room temperature at 1 °C/min [17].

2.1.2. Preparation of SiO_2–TiO_2 ceramics by sol–gel coprecipitation and hot pressing

The SiO_2–TiO_2 (ST) samples, having exactly eutectic composition (SiO_2: 89.5, TiO_2: 10.5, in wt %), were prepared starting from high purity precursors: Ti-isopropylate and tetraorthosilicate (TEOS). Appropriate amounts of the two alkoxides were mixed in ethanol under constant agitation and sealed in a water-saturated environment in order to obtain slow and controlled hydrolysis–gelation. After a few days, a perfectly transparent gel was obtained which was first dried in air at 60 °C for 2 days, then at 100 °C for 2 days and finally at 200 °C for 1 day. The resulting material, in the form of small grains, was ground for 1 h in a centrifugal ball mill with zirconia grinding media. Successively, the powder was slowly heated and calcined in air up to 600 °C to eliminate the organic compounds. Hot pressing of the samples was then carried out in a nitrogen atmosphere using a KCE hot press (Germany) with a graphite mould. A heating rate of 20 °C/min was applied and the increase in pressure was programmed in such a way as

TABLE II Physical and microstructure characteristics of mixed and single oxides

Sample	Preparation route	Density of green sample (g/cm^3) (%TD)	Density of sintered sample (g/cm^3) (%TD)	Crystallographic composition	Mean grain size (μm)
Mixed A–Z oxides					
2Z8A	slip-casting and sintering	2.61 (61)	4.25 (99.3)	(t) (α)	zirconia:0.4 alumina:0.9
4Z6A	slip-casting and sintering	2.85 (62)	4.56 (99.3)	(t) (α)	zirconia:1.0 alumina:2.0
6Z4A	slip-casting and sintering	3.04 (61)	4.96 (99.3)	(t) (α)	zirconia:0.5 alumina:1.0
8Z2A	slip-casting and sintering	2.47 (45)	5.45 (99.6)	(t) (α)	zirconia:0.5 alumina:0.6
Single oxides					
A	slip-casting and sintering	2.13 (54)	3.95 (100)	(α)	1.0
Z	slip-casting and sintering	3.08 (51)	6.05 (100)	(t)	0.6
Mixed S–T oxides					
ST1	sol–gel copre-cipitation and hot pressing		2.22	amorphous phase	
ST2	sol–gel corpre-cipitation and hotpressing		2.25	cristobalite, rutile, anatase, amorphous phase(traces)	
ST3	sol–gel corpre-cipitation and hotpressing		2.30	cristobalite, rutile	

TD:theoretical density
(α) :alpha alumina
(t) :tetragonal zirconia

to reach simultaneously the desired sintering temperatures and pressures. Different sintering conditions were applied: ST1 designates the samples sintered at 1300 °C and 13 MPa for 1 h, ST2 the samples sintered at 1350 °C and 23 MPa for 1 h and ST3 the samples sintered at 1350 °C and 23 MPa for 2 h [18].

2.2. Experimental techniques

The density of the as-cast samples was determined by the geometric method while the water immersion technique was applied for the sintered samples. The microstructure of the samples was examined using scanning electron microscopy and an image analyser. The crystal structure of the sintered samples was determined by X-ray diffraction. For the microhardness measurements, a Vickers indenter (Shimadzu microhardness tester type M, Japan) was used on polished ceramic surfaces with a finish as described later. The coefficient of linear thermal expansion was determined using a pushing rod dilatometer (Netzsch, Germany).

For the wetting experiments with biological liquids, a sessile drop technique was employed in which a liquid drop (~5 μl) was placed on a horizontal polished surface (average roughness 25 nm) of the ceramic substrate. The experiments were carried out at 37 °C and lasted for about 5 min. The liquids used were distilled water, Ringer solution (NaCl 0.8 %, KCl 0.02%, $CaCl_2$ 0.02%, $NaHCO_3$ 0.1%, pH = 7.85), ultrafiltrate calf serum (Sigma Company, frozen liquid S6648), artificial synovial fluid [19] (prepared by mixing 70 vol % Ringer solution and 30 vol% calf serum [20]), human plasma and whole human blood (with EDTA, since EDTA does not affect the physicochemical state of blood [21]). The plasma and whole blood used were fresh samples, received from healthy humans.

3. Results and discussion

3.1. Microstructure

Chemical analysis of the densified samples demonstrated that there was no measurable increase in the impurities content. However, laboratory and processing conditions can be further developed in order to eliminate more thoroughly possible contamination. For example, casting could be carried out with non-gypsum moulds to avoid potential diffusion of calcium ions into the ceramic bodies [22].

All the sintered ceramic samples were characterized by high levels of densification (Table II). The binary A–Z samples contained 0.4 to 0.7% total porosity and no open porosity. Further process improvements are in progress. The ST samples showed zero porosity.

The density of the alumina sample A (3.95 g/cm^3), satisfies the requirement of the only standard for ceramic implants in surgery ISO-6474/1992 equal to 3.94 g/cm^3.

Crystallographic characterization of the A–Z samples (Table II) showed the contemporaneous presence of the tetragonal phase of zirconia and the alpha phase

of alumina. The corresponding single crystal phases were found in the samples of the pure oxides A and Z.

SEM observations of the A–Z samples showed that all sintered samples within this series were highly homogenous and no cracks, large pores or defects were noticed, leading to the conclusion that the dispersion of the raw materials down to the colloidal level made it possible to produce uniform body structures. The alumina and zirconia grains were ideally mutually distributed, as seen in SEM micrographs of fractured surfaces such as those shown in Fig. 1 for the 2Z8A and 8Z2A samples. The SEM observations also clearly showed a perfectly homogenous and defectless microstructure of the A and Z samples, superior to that of commercially available materials.

The samples from A–Z series demonstrated two distinct ranges of grain dimensions, finer zirconia grains exclusively submicronic, and somewhat coarser alumina grains. More thorough SEM observations showed in some cases an anomalous grain growth of alumina grains [17]. Among all the materials studied, alumina sample (A) was found to be the most fine-grained one. Its grain dimensions of about 1 μm are far below the ISO-6474/1992 requirement of 4.5 μm.

The crystal structure of the ST samples is strongly affected by the sintering conditions [18, 23]. The STI samples were found to be very compact but amorphous. Small rounded areas built of very fine crystalline grains were only occasionally observed. By increasing sintering pressure and temperature (ST2), a higher degree of crystallization was obtained, however, an amorphous phase still existed. Complete crystallization was obtained only at the highest temperature and pressure employed for a long time (ST3), where well-formed crystobalite and rutile phases were found.

Fig. 2 shows SEM micrographs of the fractured surfaces of ST2 and ST3 samples. Highly homogenous microstructure and absence of pores or defects can be noticed. An abrupt increase of grain size was observed in the ST3 sample, exceeding 50 μm, whereas the grain size of the ST2 sample hardly exceeded 10 μm.

3.2. Microhardness

Microhardness measurements were carried out in air, at room temperature, with a load of 100 g and a 20 s indentation period on polished ceramic surfaces, according to the suggestions given by Buckle [24]. In polydispersed oxides the grain size (Table II) was much smaller than the indentation pattern (~ 10–15 μm). For each particular oxide, high reproducibility in the dimensions of the indentation was observed related to the high homogeneity of the samples. Cracks were not observed, probably due to the low load employed. In the case of the glassy phase containing oxides, slight but observable recovery of the indentation with time was noted, therefore the dimensions of the indentation were measured immediately after removal of the indenter.

The Vickers hardness (H_V) was calculated using the following equation:

$$H_V = 18.1916 \frac{P}{d^2} \quad \text{(GPa)} \qquad (1)$$

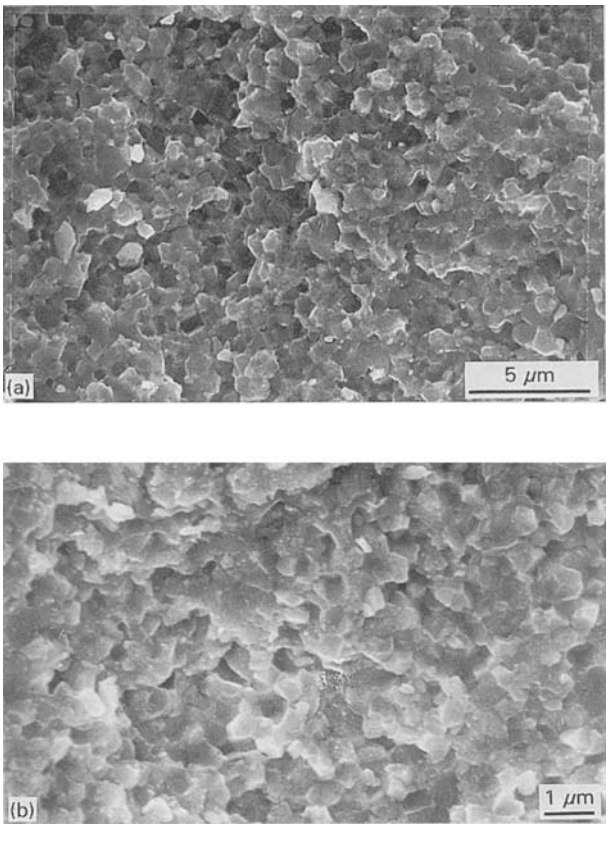

Figure 1 SEM micrographs of fractured surfaces of (a) 2Z8A and (b) 8Z2A samples (light grains: zirconia, dark grains: alumina).

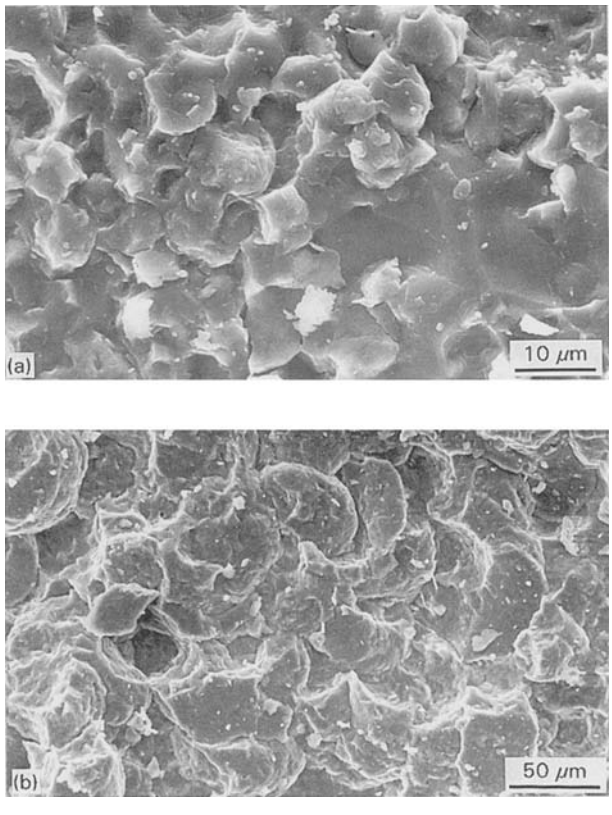

Figure 2 SEM micrographs of fractured surfaces of silica–titania samples hot-pressed at 1350 °C/23 MPa for (a) 1 h (ST2) and (b) 2 h (ST3).

where P is the load (g) and d the mean diagonal of the indentation (μm). Table III shows the mean values (± 0.1 GPa) of the Vickers hardness of the tested oxides, and, for the purposes of comparison, the measured hardness of natural tissues such as tooth enamel and bovine bone.

The values for the A (22.1 GPa) and Z (14.6 GPa) samples are in agreement with the relevant hardness values, 24.2 GPa and 14.3 GPa, respectively, found in the literature [25]. The hardness of the sample 2Z8A (25.0 GPa) is higher than that reported in the literature [25] (22.3 GPa), and even exceeds the hardness of Al_2O_3. Such behaviour can probably be attributed to the somewhat different sintering conditions (see Section 2.1.1.) as well as to the partial reinforcement of the Al_2O_3 matrix with zirconia (15 wt%) as has been described by Claussen [26].

For the SiO_2–TiO_2 samples, the measured hardness (7.5–8.0 GPa) falls in the range of hardness exhibited by SiO_2(quartz) (7.5 GPa) and TiO_2(rutile) (10 GPa) [27].

Although these values are considerably lower than those of Al_2O_3 and ZrO_2 ceramics, they are of the same order of magnitude as the hardness values of active biomaterials such as hydroxylapatite (4.5 GPa) and tricalcium phosphate (TCP) (10 GPa) [3].

The hardness of the sample of tooth enamel (3–4 GPa) is in agreement with the value of 3 GPa reported in the literature [28]. Concerning bone, there is a variety of available H_V values depending on animal, age and specific body part [29–31]. However, the H_V of bone is always much lower (< 1.5 GPa) than that of enamel, approaching the H_V of dentin (0.6 GPa) [28].

In general, microhardness data make it possible to predict the mechanical properties of both biological [29, 30] and non-living [32] materials. Considering the above data, it can be seen that all oxides tested have higher values of hardness than those of natural hard tissues. Nevertheless, it should be born in mind that human bones and teeth are made of composite materials with extraordinary mechanical strength and tolerance provided by Mother Nature.

3.3. Thermal expansion

The coefficient of thermal expansion of a material does not depend on its porosity and therefore is a good characteristic for the identification of the material. In the case of dental implants, their coefficients of thermal expansion should match well that of the bone because of the temperature changes that occur in the mouth due to the presence of food [3]. Furthermore, matching of this parameter of the two phases during fabrication of composite biomaterials (e.g. ceramic/metal [11]) can minimize the interfacial residual stresses [33].

TABLE III Measured Vickers microhardness (H_V) of the oxides and natural hard tissues

	Material	H_V (GPa)
Oxides	A	22.1
	2Z8A	25.0
	4Z6A	20.0
	6Z4A	19.0
	8Z2A	15.2
	Z	14.6
	ST1, ST2, ST3	7.5–8.0
Tissues	Tooth enamel	3–4
	Bone	0.5

The test results for the relative linear thermal expansion ($\Delta l/l_0$) of the Al_2O_3 and ZrO_2 oxides showed nearly linear temperature dependence in the range 20–1500 °C [23]. Such findings agree with the corresponding phase diagram which anticipates no phase transition in the investigated temperature range. The calculated coefficient of linear thermal expansion shifts smoothly from A to Z (Fig. 3). This observation indicates that the mixed oxides are polydispersed systems with no discontinuities in the matrix phase, in agreement with the discussion of Section 3.1.

Fig. 4 shows the dependence of $\Delta l/l_0$ on temperature of the ST3 sample. The slope of the curve perceptibly changes at about 100 °C. According to the literature, crystalline structures of silica exhibit curves of such a shape [34]. In the case of cristobalite, the change in the coefficient of thermal expansion is attributed to the transition of the lattice structure from the tetragonal to the cubic system. However, this phenomenon should be seriously taken into account in the case of dental applications such as those described above.

Table IV summarizes the calculated coefficients of linear thermal expansion α of the tested oxides. The values of the A and Z oxides agree with the literature values of Al_2O_3 ($8.1 \times 10^{-6}\ K^{-1}$) and ZrO_2 ($10.9 \times 10^{-6}\ K^{-1}$) (0–1000 °C) [35]. For the ST3 sample, the coefficient of thermal expansion changes from 16.0×10^{-6} to $3.5 \times 10^{-6}\ K^{-1}$ at about 100 °C. Both values, however, should be much higher than those of the samples containing glassy SiO_2 (ST1 and ST2). Earlier studies showed that in the range from 25 to

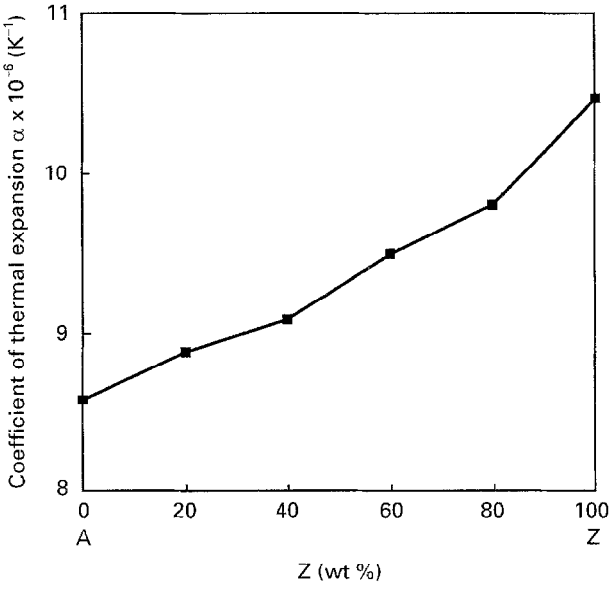

Figure 3 Coefficient of linear thermal expansion (20–1500 °C) of the Al_2O_3 and ZrO_2 oxides.

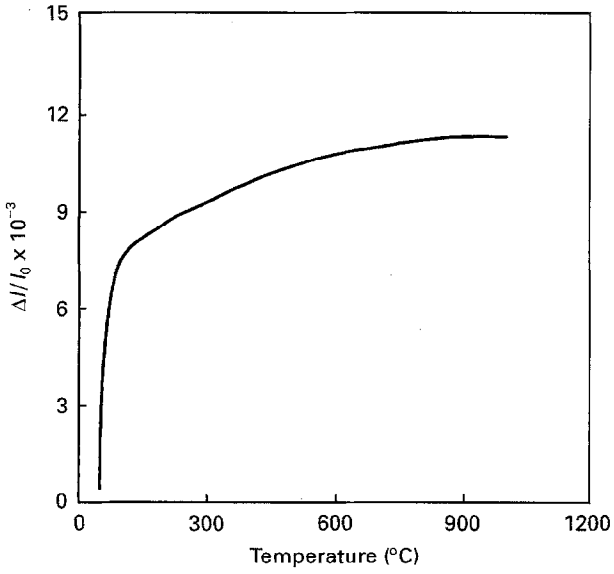

Figure 4 Relative linear thermal expansion ($\Delta l/l_0$), for the SiO_2–TiO_2 (crystalline) oxide (ST3).

TABLE IV Coefficients of linear thermal expansion (α) of the oxides tested

Oxide	$\alpha \times 10^{-6}$ (K^{-1})	
A	8.58	(20–1500 °C)
2Z8A	8.88	(20–1500 °C)
4Z6A	9.08	(20–1500 °C)
6Z4A	9.49	(20–1500 °C)
8Z2A	9.80	(20–1500 °C)
Z	10.46	(20–1500 °C)
ST3	16.0	(20–100 °C)
	3.5	(100–1000 °C)

700 °C, the behaviour of the coefficient of thermal expansion of SiO_2–TiO_2 glasses is anomalous (negative or positive), depending on the TiO_2 concentration [36–38] and heat treatment of the glass [36]. However, the maximum, observed value of α does not considerably exceed the expansion of SiO_2-glass $0.54 \times 10^{-6}\ K^{-1}$ (20–1000 °C) [35]).

Comparing the experimental α values of the oxides tested (Table IV) with those of enamel ($11.4 \times 10^{-6}\ K^{-1}$) and dentin ($8.3 \times 10^{-6}\ K^{-1}$) [3], it can be seen that pure and mixed oxides of Al_2O_3 and ZrO_2 resemble dental tissues in thermal expansion. Concerning the ceramic/metal composites, the good matching of the coefficients of thermal expansion of these oxides with that of the metal Ti ($8.9 \times 10^{-6}\ K^{-1}$, 0–100 °C), is of particular importance in biomedicine [33]. In the case of the SiO_2-containing oxides, the crystalline ones undergo a considerable change in the coefficient of thermal expansion at low temperatures, while the thermal expansion of the glassy ones differs significantly from that of dental tissues.

3.4. Wettability with body liquids – interfacial interactions

The adhesion of a biomaterial to living parts determines to a great extent the success or failure of the implantation [1]. Obviously, complete understanding of the interactions at the biomaterial/body-components interface should provide an insight about the biocompatibility of a candidate biomaterial [39] as well as ways to design new ones [6].

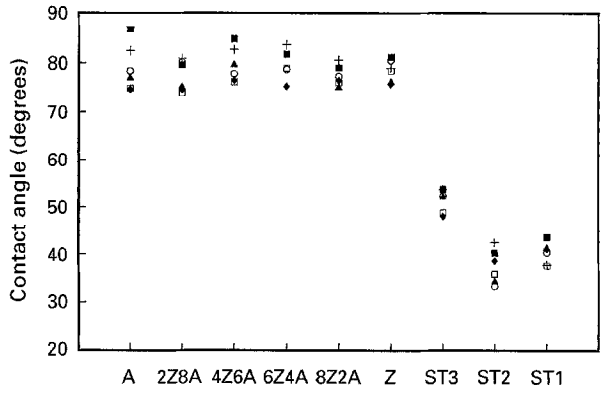

Figure 5 Contact angles in the oxide/body-liquid systems at 37 °C [40] : ■ water; + Ringer; ▲ synovial; □ serum; △ plasma; ◆blood.

Biological liquids are the first body-components which an implant faces when it is placed in the body. Furthermore, many implants maintain constant contact with these liquids during their entire lifetime [5]. In this section, the results of wetting experiments between the tested oxides and various body liquids at 37 °C are reviewed as a preliminary *in vitro* biocompatibility evaluation.

Fig. 5 shows measured contact angle values with a standard deviation of $\pm 5°$ for the investigated solid/liquid systems at 37 °C [40]. The surface homogeneity with very small grain size in polydispersed systems (Table II) compared with the liquid drop size, the absence of surface porosity and roughness, the temperature stability and the absence of any field to affect the liquid drop resulting in the constancy of the contact angle within the 5 min the experiments lasted, characterized the accuracy of the measurements. The plotted data indicate high contact angles for the Al_2O_3- and ZrO_2-containing crystalline oxides and lower contact angles for the oxides containing SiO_2. Furthermore, the presence of the glassy phase considerably improves wettability.

The work of adhesion W_a is a measure of the energy of the interfacial interactions defined as the work needed to separate reversibly the unit solid/liquid interface. In the case of the sessile drop technique, W_a can be calculated by the Young–Dupre equation:

$$W_a = \gamma_{LV}(1 + \cos\theta) \qquad (2)$$

where γ_{LV} is the surface energy of the liquid and θ the contact angle formed between the solid and the liquid.

The work of adhesion is computed by substituting in Equation 2 the contact angle data of Fig. 5 and the surface energy values of the body liquids measured by the ring method and listed in Table V. These calculations yielded values in the range 60–85 mJ/m^2 for the Al_2O_3 and ZrO_2 oxides and 80–125 mJ/m^2 for the SiO_2–TiO_2 ones. The relatively low energy upper limit of 125 mJ/m^2 indicates that the interactions at the investigated solid/liquid interfaces are due to intermolecular forces.

TABLE V Surface energies of the body liquids (γ_{LV}) and surface energies due to dispersion (γ^d) and due to polar interactions (γ^p) of the body liquids and the tested oxides at 37°C (in mJ/m^2) [40]

Liquid	γ_{LV}	γ^d_{LV}	γ^p_{LV}
Water	70.0	20.4	49.6
Ringer	70.0	20.8	49.2
Synovial	48.5	10.7	37.8
Serum	47.5	11.0	36.5
Plasma	50.5	11.0	39.5
Blood	47.5	11.2	36.3
Oxide		γ^d_{SV}	γ^p_{SV}
A		108.7	
2Z8A		86.4	
4Z6A		85.1	
6Z4A		69.3	
8Z2A		45.0	3.1
Z		53.6	2.3
ST3		107.5	3.7
ST2		72.6	15.8
ST1		45.4	37.2

In a qualitative approach, it is well known that silica glasses adhere to biological compounds better than alumina does [1, 2], which is in accordance with the calculated W_a data presented above. On the other hand, the work of adhesion between two phases with surface energies γ_1 and γ_2 can be calculated by the geometric mean law, $2(\gamma_1\gamma_2)^{1/2}$, according to the geometric model of the interface proposed by Fowkes [41] and Good and Girifalco [42]. Consequently, one would expect stronger adhesion between low surface energy biological liquids with high surface energy Al_2O_3 ($\sim$2300 mJ/m^2, at 37°C [43]) and ZrO_2 ($\sim$1300 mJ/m^2 [44]) oxides rather than with the low surface energy SiO_2-containing oxides ($\sim$370 mJ/m^2 for silica [45]). This conclusion, however, is not reflected by the experimental results, indicating that in the investigated solid/liquid systems the different types of intermolecular forces existing in the solids and the liquids do not interact with each other at the interface [41, 42].

According to this finding and assuming the same interface geometric model [41, 42], the work of adhesion can be expressed as the sum of the work of adhesion due to London-dispersion interactions, W^d_a, and the work of adhesion due to polar interactions, W^p_a, which depends on the specific chemical nature of the materials [46]:

$$W_a = W^d_a + W^p_a = 2(\gamma^d_{SV}\gamma^d_{LV})^{1/2} + 2(\gamma^p_{SV}\gamma^p_{LV})^{1/2} \quad (3)$$

where γ^d_{SV} and γ^p_{SV} denote the surface energy components of the solid due to dispersion and polar forces, respectively, and γ^d_{LV} and γ^p_{LV} the respective magnitudes for the liquid.

Table V lists the calculated values for the four surface energy magnitudes of Equation 3 determined by Agathopoulos and Nikolopoulos [40].

From the data of Table V it is obvious that the adhesion of the high surface energy oxides (Al_2O_3 and ZrO_2) to body liquids is mainly due to dispersion forces. Thereby, the other contributions to the surface energy of these oxides are of minor importance in the type of wettability studied here. This conclusion is in accordance with the low relative reactivity of alumina, classifying it as a typical inert bioceramic [1, 2].

On the other hand, when the presence of the glassy phase in the silica-containing oxides increases, the magnitude of γ^p_{SV} gives rise to the final term of Equation 3 and the polar interactions play a key role in the wettability performance. Therefore, although glasses are also classified as inert biomaterials, this result is in accordance with the known good affinity of glasses with biological substances [1, 2].

4. Conclusions

Fine microstructure candidate oxide bioceramics based on Al_2O_3 and (TZP) ZrO_2 and SiO_2–TiO_2 (of eutectic composition) were produced by slip-casting with the powders in colloidal state, followed by sintering, and by coprecipitation of the alkoxides (sol–gel) followed by hot pressing, respectively.

The pure and mixed oxides based on Al_2O_3 and ZrO_2 were fine grained, highly homogeneous and practically without porosity. Hardness increases from zirconia to Al_2O_3 and an apparent hardness maximum was observed for 20 wt% zirconia dispersed in an Al_2O_3 matrix. The coefficient of thermal expansion is constant up to 1500°C for all the compositions, shifting smoothly from pure Al_2O_3 to zirconia and matching well with that of dental tissues. The adhesion of these crystalline oxides to biological liquids is mainly due to low energy dispersion force interactions.

The microstructure of the SiO_2–TiO_2 samples depends considerably on the sintering conditions. Low Vickers hardness was measured. A significant change in the coefficient of thermal expansion at low temperatures was observed for the crystalline sample. The presence of the glassy phase in the oxides improves the affinity with biological liquids because of the action of both dispersion and polar forces at the solid/liquid interface.

Acknowledgements

The present work was carried out within the framework of the Programme EUREKA (project EU-294). The research of the Greek group was financially supported by the Greek Ministry for Industry, Energy and Technology.

References

1. L. L. HENCH and E. C. ETHRIDGE "Biomaterials–an interfacial approach" (Academic Press, New York, 1982) pp. 1–164.
2. L. L. HENCH, *J. Amer. Ceram. Soc.* **74** (1991) 1487.
3. A. F. VON RECUM "Handbook of biomaterials evaluation" (Macmillan, New York, 1986) pp. 1–72.
4. F. THUEMMLER, *J. Eur. Ceram. Soc.* **6** (1990) 139.
5. I. DION, L. BORDENAVE, F. LEFEBVRE, R. BAREILLE, C. BAQUEY, J. R. MONTIES and P. HAVLIK, *J. Mater. Sci. Mater. Med.* **5** (1994) 18.

6. D. F. WILLIAMS, *ibid.* **5** (1994) 303.
7. B. CALES, in Abstract Book of the Sixth Symposium on Biomaterials: Ceramic Implant Materials in Orthopaedic Surgery, Göttingen, 21–23 September 1994 (Orthopaedic Hospital, University of Göttingen-Germany, 1994) p. 16.
8. G. A. GOGOTSI, E. E. LAMONOVA, Y. A. FURMANOV and I. M. SAVITSKAYA, *Ceram. Int.* **20** (1994) 343.
9. W. BURGER, H. G. RICHTER, C. PICONI, R. VATTERONI, A. CITTADINI and M. BOCCALARI, in Abstract Book of the Sixth Symposium on Biomaterials: Ceramic Implant Materials in Orthopaedic Surgery, Göttingen, 21–23 September 1994 (Orthopaedic Hospital, University of Göttingen-Germany, 1994) p. 17.
10. S. LAWSON, *J. Eur. Ceram. Soc.* **15** (1995) 485.
11. G. ONDRACEK, P. NIKOLOPOULOS, I. STAMENKOVIC and E. H. TOSCANO, *Ceramica Acta* **0/89** (1989) 7.
12. R. J. BROOK, "Advances in ceramics, Vol. 12, Science and Technology of Zirconia II", edited by N. Claussen, M. Ruhle and A. Heuer (The American Ceramic Society, Ohio, 1984) p. 833.
13. J. V. NAIDICH, "Progress in surface and membrane science", Vol. 14, edited by D. A. Cadenhead and J. F. Danielli (Academic Press, New York, 1981) pp. 353–484.
14. N. EUSTATHOPOULOS and B. DREVET, *J. Physique III France* **4** (1994) 1865.
15. M. PAULASTO and J. KIVILAHTI, *Ceram. Trans.* **35** (1993) 165.
16. P. NIKOLOPOULOS and S. AGATHOPOULOS, *J. Eur. Ceram. Soc.* **10** (1992) 415.
17. A. SALOMONI, A. TUCCI, L. ESPOSITO and I. STAMENKOVIC, *J. Mater. Sci. Mater. Med.* **5** (1994) 651.
18. A. TUCCI, Internal Report in the frame of the Project Eureka (EU-294), Italian Ceramic Centre, Bologna, Italy, 1991.
19. K. DIEM and C. LENTNER "Documenta Geigy, Scientific Tables", 7th edn, (J. R. Geigy, S. A. Basel, Switzerland, 1970) pp. 640–642.
20. R. M. STREICHER, R. SCHON and M. F. SEMLITSCH, *Biomedizinische Technik* **35** (1990) 78.
21. J. V. DACIE and S. M. LEWIS "Practical haematology", 5th edn (Churchill Livingstone, Edinburgh, 1975) pp. 1–21.
22. L. ESPOSITO, A. SALOMONI, I. STAMENKOVIC and A. TUCCI, in Proceedings of the SIMCER: Special meeting on biomaterials, Rimini, 1992, edited by I. Stamenkovic and J. Krawczynski (Publ. Forschungzentrum Jülich GmbH-Germany) p. 37.
23. S. AGATHOPOULOS, PhD thesis, University of Patras, Greece, 1994.
24. H. BUCKLE, *Metall. Rev.* **4** (1959) 49.
25. A. K. IJERNLUND, L. HERMANSSON, K. ARVIDSON and R. SOREMARK, *Sci. Ceram.* **14** (1987) 799.
26. N. CLAUSSEN, *J. Amer. Ceram. Soc.* **59** (1976) 49.
27. K. H. HABIG "Verschleiß and Härte von Werkstoffen" (Carl Hanser Verlag, München Wien, 1980) p. 266.
28. H. ROELEN, Graduate Thesis, University of Karlsruhe (TH), Germany, 1985.
29. J. D. CURREY and K. BREAR, *J. Mater. Sci. Mater. Med.* **1** (1990) 14.
30. G. P. EVANS, J. C. BEHIRI, J. D. CURREY and W. BONFIELD, *ibid.* **1** (1990) 38.
31. S. STEA, C. TARABUSI, G. CIAPETTI, A. PIZZOFERRATO, A. TONI and A. SUDANESE, *ibid.* **3** (1992) 252.
32. K. SHINOHARA, *J. Mater. Sci.* **28** (1993) 5325.
33. J. EMILIANO, PhD thesis, University of Aveiro, Portugal, 1996.
34. H. SALMANG and H. SCHOLZE "Keramik" (Springer Verlag, Berlin, 1982) pp. 38, 187, 191.
35. J. F. LYNCH, C. G. RUDERER and W. H. DUCKWORTH "Engineering properties of selected ceramics materials" (The American Ceramic Society, Columbus, OH, 1966) pp. 5.4.1–6.
36. P. C. SCHULTZ, *J. Amer. Ceram. Soc.* **59** (1976) 214.
37. K. KAMIYA and S. SAKKA, *J. Mater. Sci.* **15** (1980) 2937.
38. T. HANADA, T. AIKAWA and N. SOGA, *J. Amer. Ceram. Soc.* **67** (1984) 52.
39. D. F. WILLIAMS, *J. Biomed. Engng.* **11** (1989) 185.
40. S. AGATHOPOULOS and P. NIKOLOPOULOS, *J. Biomed. Mater. Res.* **29** (1995) 421.
41. F. M. FOWKES, *Ind. Engng. Chem.* **56** (1964) 40.
42. R. J. GOOD and L. A. GIRIFALCO, *J. Phys. Chem.* **64** (1960) 561.
43. P. NIKOLOPOULOS, *J. Mater. Sci.* **20** (1985) 3993.
44. D. SOTIROPOULOU and P. NIKOLOPOULOS, *ibid.* **26** (1991) 1395.
45. P. NIKOLOPOULOS and G. ONDRACEK "Verbundwerkstoffe" (Deutsche Gesellschaft für Metallkunde, Oberursel, 1981) pp. 391–407.
46. D. K. CHATTORAJ and S. K. BIRDI "Adsorption and the Gibbs surface excess" (Plenum Press, New York, 1984) pp. 233–256.

Received 5 January
and accepted 30 November 1995